

INDUCED THETA VACUA IN HEAVY ION COLLISIONS

By

Kirk B.W. Buckley

B. Sc., Bishop's University, 1998

A THESIS SUBMITTED IN PARTIAL FULFILLMENT OF
THE REQUIREMENTS FOR THE DEGREE OF
MASTER OF SCIENCE

in

THE FACULTY OF GRADUATE STUDIES
DEPARTMENT OF PHYSICS AND ASTRONOMY

We accept this thesis as conforming
to the required standard

THE UNIVERSITY OF BRITISH COLUMBIA

June 2000

© Kirk B.W. Buckley, 2000

In presenting this thesis in partial fulfilment of the requirements for an advanced degree at the University of British Columbia, I agree that the Library shall make it freely available for reference and study. I further agree that permission for extensive copying of this thesis for scholarly purposes may be granted by the head of my department or by his or her representatives. It is understood that copying or publication of this thesis for financial gain shall not be allowed without my written permission.

Department of Physics and Astronomy
The University of British Columbia
6224 Agricultural Road
Vancouver, B.C., Canada
V6T 1Z1

Date:

June 12, 2000

Abstract

In the following we demonstrate that it is possible to create non-zero θ -states during heavy ion collisions. Using the effective Lagrangian for low energy QCD derived in [1, 2], we will show numerically that in the period immediately following a quench, the chiral condensate phases ϕ_u and ϕ_d will relax to the value $\sim \theta/N_f$. This is a true condensate in the sense that if the volume of the system is changed, the zero mode still remains. If such a state can be created, it would decay by various mechanisms to the $\theta^{fund} = 0$ state which exists in our world. We will discuss the experimental signature for the produced non-trivial θ -state. In particular, we will provide evidence that the creation of a non-zero θ -state would result in an excess of low momentum particles (π^0 , η , and η' -mesons), in the $(10 - 100)$ MeV range. This phenomena could possibly account for the excess of low momentum dileptons observed at CERN [3, 4].

Table of Contents

Abstract	ii
Table of Contents	iii
List of Figures	v
Acknowledgements	vii
1 Introduction	1
1.1 Review of Quantum Chromodynamics and the θ Term	2
1.2 Overview	8
2 Effective Lagrangians and QCD	10
2.1 A Simple Example: the Linear Sigma Model	10
2.2 Di Vecchia-Veneziano-Witten Effective Chiral Lagrangian	11
2.3 Halperin-Zhitnitsky Anomalous Effective Chiral Lagrangian	13
3 Induced Theta Vacua	18
3.1 What is the difference between θ^{ind} and the fundamental θ parameter?	19
3.2 Disoriented Chiral Condensate	20
3.3 θ -State in Heavy Ion Collisions	21
3.4 Evolution of the Equations of Motion	24
4 Signatures of an Induced θ-Vacuum State	29
4.1 Properties of the pseudo-Goldstone Bosons in the non-zero θ -Background	30

4.2	Signature of the Creation of θ -Vacua	31
4.3	Results	34
5	Conclusions and Future Considerations	42
	Bibliography	44

List of Figures

3.1	$ \phi_k $ is shown for various $ \vec{k} $ as a function of time. In a time $\sim 10^{-23}$ sec, the zero mode relaxes to $\bar{\phi}_i \sim \theta/N_f$ and all other modes decay to zero. This is very similar to the idea of a disoriented chiral condensate.	26
3.2	Above we demonstrate that the system exhibits the coarsening phenomenon (amplification of the zero mode as time increases). The data was sampled at three times within the first 1000 time steps of the evolution.	26
3.3	The zero mode and a non-zero mode are shown as a function of time for three different volumes. The heavily dashed line represents the smallest volume $(8 \text{ fm})^3$, the medium dashed line represents the middle volume $(16 \text{ fm})^3$, and the solid line represents the largest volume $(32 \text{ fm})^3$. The volume independence of the zero mode reinforces the claim that a true nonperturbative condensate has been formed.	27
4.1	$ \phi_i(k=0) $ is plotted as a function of time for the up, down, and strange quark. Notice that the zero momentum modes of the ϕ_i fields settle to a non-zero value in a time on the order of 10^{-23} s. The times t_1 and t_2 represent the value we chose for τ_{shell} , the the time when the shell separating the two regions disappears.	35

4.2	We plot the number of pions produced, $N_{\pi^0}(k)$ as a function of the magnitude of the wave vector, $ \vec{k} $. Above we show that the momentum distribution of the π^0 -mesons produced is primarily $< 25 \text{ MeV}$ for two different values of τ_{shell} . The solid line represents the earlier time t_1 and the dotted line represents the later time t_2 (see Fig. 4.1 for the positions of t_1 and t_2 in the evolution of the ϕ_i fields). This is expected as the formation of the θ -state can be attributed to the enhancement of the low momentum modes.	36
4.3	$N_{\eta}(K)$ is plotted as a function $ \vec{k} $, at two different times t_1 and t_2 as in Fig. 4.2. The higher peak represents the later time with the main difference being that now a larger percentage of the produced particles lie in the $k < 25 \text{ MeV}$ range.	37
4.4	$N_{\eta'}(k)$ vs. $ \vec{k} $ is shown above. This graph shows that the η' clearly dominates the spectrum compared to the other neutral particles.	38
4.5	The momentum distribution ($N_{\eta'}(k)$ vs. $ \vec{k} $) is now shown for the case where the geometry of the θ -region is considered as a rectangle. We consider the case where the size of the θ -region is larger along the longitudinal directions compared to the transverse directions. The solid and dotted lines once again represent times $\tau_{shell} = t_1$ and t_2 respectively. Although the majority of the spectrum still exists in the low momentum range, the higher momentum modes now become more evident.	40
4.6	For the scenario shown in Fig. 4.5, we consider the angular dependence on the azimuthal angle for the π^0 instead of the η' . The azimuthal angle is defined so that $\theta = 0$ coincides with the beam axis.	41

Acknowledgements

I would like to thank several people for their help along the way. I would like to thank my supervisor Ariel Zhitnitsky for providing a sense of enthusiasm, ideas, and for his patience in answering a seemingly infinite number of questions. I would also like to extend my gratitude to Nathan Weiss for useful discussions, as well as Konstantin Zarembo for reading over this thesis.

My friends that I have met while at U.B.C., Todd , Matt , and Mark, have made my time here quite enjoyable as well as always being available for discussions and input. I would also like to thank my collaborator Todd Fugleberg for working with me over the last year. Finally, I am grateful to my family and Lauren for their constant support and encouragement throughout the course of this work.

Chapter 1

Introduction

Over the past 30 years the theory of quantum chromodynamics (QCD) has been universally accepted as the description of the strong force. The theory has been tested experimentally with great precision in accelerator experiments. Although the Lagrangian of the theory is well known, there are still many mysteries which surround QCD. With the advent of modern heavy ion colliders, such as the Relativistic Heavy Ion Collider (RHIC) at Brookhaven National Laboratory, it may be possible to answer many of these pending questions. The hope is that in these colliders it may be possible to indirectly observe a plasma of quarks and gluons, which is thought to have existed at the beginning of the universe. This could signify the creation of a new form of quark matter at high temperature and large chemical potential. The study of QCD under extreme conditions has been the subject of extensive research in the last few years. One of the most exciting ideas is that at high densities and low temperatures such as the interior of neutron stars, quark matter could take on a superconducting phase where a condensate of quark-quark pairs would form. In the following we provide evidence that an additional induced θ -state could be observed in heavy ion collisions. This could be very exciting as it has been verified experimentally that $|\theta^{fundamental}| < 10^{-9}$. We will also provide suggestions of experimental signatures that can be observed in order to verify that such a non-trivial vacuum state has been created.

1.1 Review of Quantum Chromodynamics and the θ Term

The spectrum of QCD consists of six flavors of fermions (quarks) and eight vector bosons (gluons) which are the mediators of the strong force. In addition to the characteristic quantum numbers of a spin 1/2 fermion, the quarks carry an additional quantum number, color charge. There are six different flavors of quarks with each one having a distinct charge and mass. The quarks are represented by $\psi^{\alpha k}$, where $\alpha = up, down, strange, charm, bottom, top$ is the flavor index and $k = 1, 2, 3$ is the color index. The gluons also carry color charge and are represented by the field A_μ^a with $a = 1, 2, \dots, 8$ being the color index and μ the usual Lorentz index. The Lagrangian of the theory is given by the following equation:

$$\mathcal{L}_{QCD} = -\frac{1}{4}G_{\mu\nu}^a G_{\mu\nu}^a + \sum_{\alpha=1}^{N_f} \bar{\Psi}^{\alpha j} (i\gamma_\mu D_\mu^{jk} + m^\alpha \delta^{jk}) \Psi^{\alpha k} + \theta \frac{g^2}{64\pi^2} G_{\mu\nu}^a \tilde{G}_{\mu\nu}^a, \quad (1.1)$$

where g is the coupling constant. The first term of Eq.(1.1) is the kinetic term of the gluon, otherwise known the gluon field strength tensor, the second term represents the kinetic term of the quark and the quark-gluon interaction, with the covariant derivative $D_\mu = \partial_\mu + igA_\mu^a \frac{\lambda^a}{2}$, and the third term represents an anomaly which does not appear at any order in perturbation theory (this will be discussed in more detail shortly). The gauge group for the color charge is $SU(3)$ with the generators represented by λ^a and a set of corresponding structure constants given by f^{abc} . The generators of the gauge group obey the following commutation relations:

$$\left[\frac{\lambda^a}{2}, \frac{\lambda^b}{2} \right] = if^{abc} \frac{\lambda^c}{2}. \quad (1.2)$$

The gauge field can be written as $A_\mu = A_\mu^a \frac{\lambda^a}{2}$. Using the commutation relations given in Eq.(1.2), the field strength tensor $G_{\mu\nu}^c$ is given by the following:

$$G_{\mu\nu}^c = G_\mu^c \frac{\lambda^c}{2} = \partial_\mu A_\nu - \partial_\nu A_\mu - ig[A_\mu, A_\nu]$$

$$= (\partial_\mu A_\nu^c - \partial_\nu A_\mu^c + gf^{abc}A_\mu^a A_\nu^b) \frac{\lambda^c}{2}, \quad (1.3)$$

which implies that

$$G_\mu^c = \partial_\mu A_\nu^c - \partial_\nu A_\mu^c + gf^{abc}A_\mu^a A_\nu^b. \quad (1.4)$$

The dual field strength tensor is given by $\tilde{G}_{\mu\nu} = \epsilon_{\sigma\rho\mu\nu} G_{\sigma\rho}$, with $\epsilon_{\sigma\rho\mu\nu}$ the totally anti-symmetric four index tensor. Due to the non-Abelian nature of the $SU(3)$ gauge group of QCD, the commutator in the first line of Eq.(1.3) does not vanish and therefore leads to a self-coupling between gluons. This complicates matters greatly by allowing the creation of virtual gluon pairs. Consequently, if one wishes to calculate a diagram containing a virtual fermion-antifermion pair, the corresponding Feynman diagram with a gluon pair included must also be calculated.

Although the QCD Lagrangian given in Eq.(1.1) at first glance looks similar to the equations of other well known theories such as the electroweak theory, it contains many unique features. The first of these is the property of asymptotic freedom. This means that contrary to quantum electrodynamics or classical gravity, the coupling constant g grows larger when we go to large distances or conversely, small momenta. Using the renormalization group equation, $\alpha_s = \frac{g^2}{4\pi}$ is given as a function of Q according to the following equation:

$$\alpha_s(Q) = \frac{2\pi}{b_0 \log(Q/\Lambda_{QCD})}, \quad (1.5)$$

where Λ_{QCD} is the momentum scale at which α_s becomes strong as Q is decreased and the constant $b_0 = 11 - \frac{2}{3}N_f$, with N_f the number of quarks flavors being considered. Current experimental measurements indicate that $\Lambda_{QCD} \approx 200MeV$. This is what essentially sets the characteristic energy scale of the strong force. One of the consequences of this is that quarks are essentially free inside baryons. This is somewhat counterintuitive as the strength of the gravitational and electromagnetic forces are inversely proportional to the distance. Due to the spontaneous creation of charged fermion-antifermion pairs

in the QED vacuum, we know that electric charge is screened. In QCD, we have the opposite situation where color charge is antiscreened. The QCD vacuum receives similar effects from quark-antiquark pairs, but these are suppressed by contributions from virtual gluons.

In addition to asymptotic freedom, QCD also exhibits confinement of color. That is, only finite-energy asymptotic states of the theory exist as color neutral combinations of quarks. The consequence of confinement is that the experimental observation of a solitary quark is forbidden. For example, if we tried to pull an up quark out of a proton (2 up quarks, 1 down quark), a pair of quarks would be created leaving us with a pion and a neutron. Although there is no current theoretical proof for confinement derived from ordinary QCD, all experiment evidence obtained so far points to this.

The unique features of QCD definitely do not end with confinement. We know that the QCD vacuum is filled with a condensate of quark-antiquark pairs. In other words, the following quantity has a non-zero vacuum expectation value:

$$\langle 0 | \bar{\psi} \psi | 0 \rangle = \langle 0 | \bar{\psi}_L \psi_R | 0 \rangle + \langle 0 | \bar{\psi}_R \psi_L | 0 \rangle, \quad (1.6)$$

which means that we lose the freedom to freely rotate left handed quarks independent of right handed quarks. This phenomenon is referred to as dynamical chiral symmetry breaking. The Lagrangian possesses this chiral symmetry (with $m_q = 0$) but the vacuum does not share a similar property. The chiral condensate given in Eq.(1.6) can be calculated by using so called soft-pion techniques to give $\langle \bar{\psi} \psi \rangle = -(240 \text{ MeV})^3$.

The QCD Lagrangian with all quark masses set to zero is invariant under the large symmetry group $SU(3)_{color} \times SU(3)_{right} \times SU(3)_{left} \times U(1)_b \times U(1)_a \times R_{scale}$, but this is broken down to $SU(3)_{left+right} \times U(1)_b$ by various mechanisms. In the unbroken symmetry group, $SU(3)_{color}$ is the gauge group for the gluons, $SU(3)_{right}(SU(3)_{left})$ is the

freedom to freely rotate right-handed (left-handed) among one another, $U(1)_b$ corresponds to baryon number (common phases for all quark fields), $U(1)_a$ is axion baryon number (equal and opposite phases for all left-handed and right-handed quark fields), and R_{scale} corresponds to scale invariance. The color symmetry is hidden by the confinement phenomenon. The $SU(3)_{right} \times SU(3)_{left}$ is broken down to $SU(3)_{left+right}$ by dynamical chiral symmetry breaking. Conservation of axial baryon number is violated through the triangle anomaly or chiral anomaly. Finally, the running of the coupling constant or asymptotic freedom breaks scale invariance. Although there does not exist conclusive evidence, lattice calculations indicate that a chiral symmetry restoration/deconfinement phase transition occurs at a temperature of about $T_c \simeq 150 \text{ MeV}$.

In Eq.(1.1), the last term $\theta \frac{g}{64\pi^2} G_{\mu\nu}^a \tilde{G}_{\mu\nu}^a$ is connected with the non-trivial vacuum structure of QCD as well as the chiral anomaly. This term is very important to this thesis, so we will give a brief explanation of its origin (for a more detailed explanation, see [5]).

It can be shown that there is a conserved quantity, called the winding number n , which is characteristic of all gauge potentials A_μ . It is defined as:

$$n = \frac{ig^3}{24\pi^2} \int d^3x \text{Tr}(A_i(x)A_j(x)A_k(x))\epsilon_{ijk}. \quad (1.7)$$

If we consider the integral:

$$Q = \int d^4x \frac{g^2}{64\pi^2} G_{\mu\nu}^a \tilde{G}_{\mu\nu}^a = n_2 - n_1 = \nu, \quad (1.8)$$

we see that it is actually the difference between winding numbers n_i . The quantity Q is referred to as the topological charge. This is surprising as the integrand can be rewritten as a total derivative:

$$\partial_\mu K_\mu = G_{\mu\nu}^a \tilde{G}_{\mu\nu}^a \quad (1.9)$$

with

$$K_\mu = 2\epsilon_{\mu\nu\beta\gamma}A_\nu^a(G_{\beta\gamma}^a - \frac{g}{6}f^{abc}A_\beta^bA_\gamma^c) \quad (1.10)$$

Naively, we should assume that since this is a total derivative we can integrate the action by parts and discard this term as it is merely a surface term evaluated at $x_\mu = \pm\infty$. This is simply not true as the different winding numbers actually belong to different homotopy classes. In other words, one gauge field configuration cannot be continuously deformed into another if their respective winding numbers are different. Gauge invariance implies that the QCD vacuum must receive contributions from all homotopy classes and is a coherent superposition of all winding states:

$$|\theta\rangle = \sum e^{-in\theta}|n\rangle, \quad (1.11)$$

where θ is the QCD vacuum label. To see how the Lagrangian must be modified in order to take into account the non-trivial vacuum structure, we consider the following matrix element of an arbitrary operator X :

$$\langle\theta|X|\theta\rangle = \sum_{m,n} e^{i(m-n)\theta}\langle n|X|m\rangle. \quad (1.12)$$

Notice that the path integral acquires an extra phase ($m - n$ is just the difference in winding states). In order to properly take into account this phase when doing calculations we must add to the QCD Lagrangian the θ -term:

$$\mathcal{L}_{QCD} \rightarrow \mathcal{L}_{QCD} + \theta \frac{g^2}{64\pi^2} G_{\mu\nu}^a \tilde{G}_{\mu\nu}^a. \quad (1.13)$$

Now we will discuss the connection between θ vacua and the axial anomaly. If we consider Eq.(1.1) as a classical field theory, then Noether's theorem tells us that the axial current is a conserved current:

$$j_{5\mu}^{(0)} = \bar{u}\gamma_\mu\gamma_5u + \bar{d}\gamma_\mu\gamma_5d + \bar{s}\gamma_\mu\gamma_5s, \quad (1.14)$$

ie. $\partial_\mu j_{5\mu}^{(0)} = 0$ in the chiral limit where all quark masses vanish. Upon quantization, this current is no longer a conserved current of the theory as it receives quantum corrections. In order to see that the axial current is not divergenceless, the famous triangle diagram must be calculated. When this calculation is done, we see that the chiral current has an anomaly given by:

$$\partial_\mu j_{5\mu}^{(0)} = \frac{N_f \alpha_s}{8\pi} G_{\mu\nu}^a \tilde{G}_{\mu\nu}^a \quad (1.15)$$

The only way to ensure that the axial current is conserved is to add to $j_{5\mu}^{(0)}$ an extra term given by Eq.(1.10):

$$j_{5\mu}^{(0)} \rightarrow \tilde{j}_{5\mu}^{(0)} = j_{5\mu}^{(0)} - \frac{N_f \alpha_s}{8\pi} K_\mu \quad (1.16)$$

By performing a gauge transformation of the conserved charge $\tilde{Q}_5 = \int d^3x \tilde{j}_{5,0}^{(0)}$, we see that the different $|\theta\rangle$ vacua are related by a chiral $U(1)_A$ transformation:

$$e^{i\alpha\tilde{Q}_5} |\theta\rangle = |\theta - 2N_f\alpha\rangle \quad (1.17)$$

where α is an arbitrary constant.

The actual θ parameter that appears in the QCD Lagrangian receives contributions from two different sources:

$$\theta = \theta_{QCD} + \arg(\det M), \quad (1.18)$$

where the first term is the QCD vacuum label and the second term is introduced upon diagonalization of the quark mass matrix, M . If θ is non-zero in Nature, then one should observe a magnetic dipole moment for the neutron. This has been measured experimentally and results indicate that the two contributions in Eq.(1.18) cancel to precision better than 10^{-9} . The strong CP problem asks why these two terms should cancel with such high precision (see [6] for a recent review). One possible solution to the strong CP problem is to promote the θ parameter to a dynamical field to represent a theoretical particle called the axion (for further details regarding axion physics see

[7, 8, 9]). If this proves to be true, it provides a solution for the strong CP problem as well as accounting for some of the unexplained dark matter in the universe.

We would also like to note that if the θ -parameter possesses a non-zero value, the P and CP symmetries are strongly violated. This comes from the fact that the θ -parameter comes into the equations with the anti-symmetric four index tensor $\epsilon_{\sigma\rho\mu\nu}$ which breaks parity invariance. The vacuum state with $\theta \neq 0$ is a stable ground state when one works in the thermodynamic limit ($V \rightarrow \infty$). If one considers only gauge-invariant observables \mathcal{O} in QCD, it is well known that there are no transitions between two distinct θ -vacua as $\langle \theta | \mathcal{O} | \theta' \rangle \sim \delta(\theta - \theta')$ [10, 11, 12].

1.2 Overview

This thesis is organized in the following manner. In Chapter 2, we introduce the effective Lagrangian approach. We will present the well known linear sigma model as a simple example that is used frequently to model low energy QCD. Next, we will briefly review the large N_c Di Vecchia-Veneziano-Witten effective Lagrangian for QCD as given in [13, 14, 15, 16]. The anomalous effective chiral Lagrangian (ECL) constructed by Halperin and Zhitnitsky [1, 2] represents an improvement to the potential given in [13, 14, 15, 16], as it is valid for finite N_c . We will concentrate on this as all calculations that follow will rely upon it.

In Chapter 3, the motivation for studying an induced θ -state is presented. It is crucial to clarify the difference between a non-zero θ^{ind} -state and a non-zero $\theta^{fundamental}$ -state. We will also present a strong analogy between the creation of a non-zero θ^{ind} -state in heavy ion collisions and the possibility of observing disoriented chiral condensate(DCC). The idea of a DCC in heavy ion collisions has been studied extensively over the past ten years [17, 18, 19, 20, 21]. Chapter 3 will be concluded with results from a numerical

simulation that support the possibility of the creation of a θ^{ind} -state in heavy ion collisions [22].

As we will see in Chapter 4, the physics of this world is very different from our world with $\theta = 0$. The properties of the Goldstones Bosons are altered [23, 24] and CP (charge conjugation times parity) is no a longer valid symmetry of the system. Furthermore, there will be an excess of low momentum particles (in the (10-100) MeV range) as our calculations demonstrate [25].

We conclude this thesis in Chapter 5 with a summary of our results and future considerations.

Chapter 2

Effective Lagrangians and QCD

In certain circumstances, the full field theory which incorporates all degrees of freedom may be unnecessary. When these situations arise, it is convenient to define an effective Lagrangian which represents the dynamics of the low energy degrees of freedom. The effective Lagrangian is obtained by integrating the heavy particles out of the full action and incorporating their effects into a few simple constants. Effective Lagrangian techniques have proven to be extremely useful in practically all areas of physics, from particle physics to condensed matter physics.

In order to study the vacuum structure of QCD, we must consider the low energy regime ($E < \Lambda_{QCD} \approx 200 \text{ MeV}$). This is a theory that is highly nonperturbative and we must formulate a new plan of attack. We are now presented with an ideal setting to use effective Lagrangian techniques. In the following few sections we will describe various effective Lagrangians which are relevant to the calculations presented in this thesis.

2.1 A Simple Example: the Linear Sigma Model

We will begin with a well known field theory model, the linear sigma model. This theory was an early candidate for QCD which described the dynamics of a doublet of nucleons (proton and neutron), a triplet of pions (π^+ , π^0 , and π^-), and a scalar field σ . The Lagrangian is constructed so that $SU(2)_L \times SU(2)_R$ is a symmetry of the theory:

$$\begin{aligned} \mathcal{L} = & \bar{\psi} i \gamma_\mu \partial_\mu \psi + \frac{1}{2} \partial_\mu \vec{\pi} \cdot \partial_\mu \vec{\pi} + \frac{1}{2} \partial_\mu \vec{\sigma} \partial_\mu \vec{\sigma} - g \bar{\psi} (\sigma - i \vec{\tau} \cdot \vec{\pi} \gamma_5) \psi \\ & + \frac{\mu^2}{2} (\sigma^2 + \vec{\pi}^2) - \frac{\lambda}{2} (\sigma^2 + \vec{\pi}^2)^2, \end{aligned} \quad (2.1)$$

with

$$\psi = \begin{pmatrix} p \\ n \end{pmatrix}, \quad (2.2)$$

$$\vec{\pi} = (\pi^1, \pi^2, \pi^3), \quad (2.3)$$

and $\vec{\tau} = (\tau^1, \tau^2, \tau^3)$ the three Pauli matrices. The scalar σ field represents the chiral condensate, Eq.(1.6). Upon minimizing the potential in Eq.(2.1), we see that the vacuum expectation value of the $\vec{\pi}$ and σ fields are:

$$\langle \vec{\pi} \rangle = 0, \quad \langle \sigma \rangle = \sqrt{\frac{\mu^2}{\lambda}} = v, \quad (2.4)$$

and the chiral condensate has a non-zero vacuum expectation value, as desired in order to model QCD. Considering only low energy physics, below the scale of the m_π , all the matrix elements that can be calculated using Eq.(2.1) can be incorporated into the following effective Lagrangian:

$$\mathcal{L}_{eff} = \frac{F^2}{2} Tr(\partial_\mu U \partial^\mu U^\dagger), \quad U = \exp(i \vec{\tau} \cdot \vec{\pi} / F), \quad (2.5)$$

with $F = v$ from Eq.(2.4) to first order in the coupling constant. In order to calculate any pion scattering amplitudes, we can expand U in powers of pion field, $U = \exp(i \vec{\tau} \cdot \vec{\pi} / F) \simeq 1 + i \vec{\tau} \cdot \vec{\pi} / F$.

2.2 Di Vecchia-Veneziano-Witten Effective Chiral Lagrangian

Next, we will briefly review the Di Vecchia-Veneziano-Witten effective chiral Lagrangian as given in [13, 14, 15, 16]. In these papers, they begin by constructing the most general

equation due to symmetry arguments alone. In the low energy limit, we know that the theory must possess the following properties:

1. In the large N_c limit, QCD exhibits confinement and chiral symmetry breaking.
2. In the case of three flavors of light quarks with $m_q = 0$, we have a $U(3) \times U(3)$ chiral symmetry in the limit $N_c \rightarrow \infty$. Because of chiral symmetry breaking, this is broken down to $U(3)$ spontaneously and there is a nonet of pseudo-Goldstone bosons¹ which consists of the π -mesons, K -mesons, η , and the η' .
3. The axial anomaly is proportional to $1/N_c$ and is therefore absent in the large N_c limit.

In order to describe the lowest energy particles of the theory in a world with 3 flavors of quarks, we parameterize the pseudo-Goldstone bosons by a 3×3 unitary matrix $U = U_o(1 + i \sum t^a \pi^a / F_\pi + \mathcal{O}(\pi^2))$, where U_o is the vacuum expectation value of U , t^a are the generators of the group $U(3)$, and π^a represents the Goldstone bosons. The constant F_π is the pion decay constant, $F_\pi = 93 \text{ MeV}$. In order for the Lagrangian to correctly transform under a $U(3) \times U(3)$ transformation $U \rightarrow AUB^\dagger$, with A and B^\dagger arbitrary unitary 3×3 matrices, there are only a limited number of terms which can be introduced. The kinetic term must assume the form $Tr(\partial_\mu U \partial_\mu U^{-1})$ and the mass term the form $Tr(\mathcal{M}U + \mathcal{M}^\dagger U^\dagger)$, with \mathcal{M} a 3×3 matrix which is proportional to the quark mass matrix. In principle, higher order derivative terms could be included, but these can all be neglected in the low energy limit. In [13, 14, 15, 16], it was also pointed out that the axial anomaly breaks $U(3) \times U(3)$ but preserves $SU(3) \times SU(3)(\times U(1))$. Obeying the above constraints, the effective Lagrangian is given as follows:

$$\mathcal{L} = \frac{F_\pi^2}{2} \left(Tr \partial_\mu U \partial_\mu U^{-1} + Tr(\mathcal{M}U + \mathcal{M}^\dagger U^\dagger) - \frac{a}{N} (-i \ln \det U)^2 \right), \quad (2.6)$$

¹In the chiral limit where all quark masses vanish, there would be a nonet of true massless Goldstone bosons.

where a is a constant of order one and the constant F_π is included to ensure that the action is a dimensionless quantity. We can diagonalize the matrix \mathcal{M} by an $SU(3) \times SU(3)$ transformation $\mathcal{M} = e^{i\theta/3} M$. We are also free to perform the following transformation, $U \rightarrow e^{-i\theta/3} U$ and therefore $\ln \det U \rightarrow \ln \det U - i\theta$. Once this is implemented in Eq.(2.6), we are left with:

$$\mathcal{L} = \frac{F_\pi^2}{2} \left(\text{Tr} \partial_\mu U \partial_\mu U^{-1} + \text{Tr}(MU + MU^\dagger) - \frac{a}{N} (-i \ln \det U - \theta)^2 \right). \quad (2.7)$$

The VVW effective Lagrangian describes the light matter fields of QCD and incorporates the QCD vacuum angle θ , as well as the axial anomaly. This can be used to calculate various meson amplitudes to lowest order as well as allowing the vacuum structure of QCD to be studied.

2.3 Halperin-Zhitnitsky Anomalous Effective Chiral Lagrangian

The Di Vecchia-Veneziano-Witten effective Lagrangian has proven to be very useful in the past in explaining such phenomena as the $U(1)$ problem. The $U(1)$ problem asks why the η' -meson so much heavier than the octet of pseudo-Goldstone bosons. As was demonstrated by Halperin and Zhitnitsky (HZ) in [1, 2], the VVW effective potential could be improved upon. The improvements included the potential being valid for a finite number of colors, N_c , and the quantization of the topological charge being explicitly incorporated from the beginning. The HZ anomalous effective chiral Lagrangian can be further tested by showing that it reproduces the anomalous conformal and chiral Ward identities of QCD and can be expanded to reproduce the large N_c Di Vecchia-Veneziano-Witten effective chiral Lagrangian plus corrections proportional to $1/N_c$.

Usually there are two definitions of an effective Lagrangian. One is the Wilsonian effective Lagrangian which describes the low energy dynamics of the lightest particles in the theory and the other is defined as the Legendre transform of the generating functional

for connected Green functions. The VVW effective potential is of the former type in that it describes only the lightest particles in the theory (the Goldstone bosons), but it also incorporates the effects of the chiral anomaly. In deriving their Lagrangian, HZ take the generating functional approach and arrive at the Wilsonian effective Lagrangian upon integrating out the massive “glueball” fields. We will now briefly summarize the steps that were taken in order to arrive at the improved effective potential for low energy QCD (see [1] and [2] for a more complete description).

The construction of the Lagrangian starts off with imposing that the anomalous conformal and chiral Ward identities of QCD hold at the tree level. Once consistency with the anomalous Ward Identities is ensured, the light matter fields of the theory, which are parameterized by a $N_f \times N_f$ unitary matrix U , are introduced by the substitution:

$$\theta \rightarrow \theta - iT r \log U. \quad (2.8)$$

The chiral anomaly dictates the exact form of the above substitution. If we consider $N_f = 3$ flavors of quarks, the light matter fields consist of an octet of pseudo-Goldstone bosons (π 's, K 's, and the η) and the η' singlet field. The mass term for the U field remains unchanged from the arguments given in the previous section for the VVW potential. The unitary matrix U_{ij} corresponds to the γ_5 phases of the chiral condensate, $\langle \bar{\Psi}_R^i \Psi_L^j \rangle = -|\langle \bar{\Psi}_R \Psi_L \rangle| U_{ij}$, and takes the following form:

$$U = \exp \left[i\sqrt{2} \frac{\pi^a \lambda^a}{f_\pi} + i \frac{2}{\sqrt{N_f}} \frac{\eta'}{f_{\eta'}} \right], \quad (2.9)$$

where U_0 is the vacuum expectation value of the U field, π^a represents the pseudoscalar octet, N_f is the number of flavors, λ^a are the generators for $SU(N_f)$, and the constants $f_\pi = F_\pi \sqrt{2} = 133 \text{ MeV}$ and $f_{\eta'} = 86 \text{ MeV}$. Upon integrating out the heavy “glueball” fields, the potential for the U field is given by the following expression [1, 2]:

$$V(U, \theta) = - \lim_{V \rightarrow \infty} \frac{1}{V} \log \sum_{l=0}^{N_c-1} \exp(V E \cos \left(\frac{1}{N_c} (\theta - i \log \text{Det} U + \frac{2\pi}{N_c} l) \right))$$

$$+ \frac{1}{2} V \text{Tr}(MU + M^\dagger U^\dagger) \quad (2.10)$$

where V is the 4-volume, $M = -\text{diag}(m_i \langle \bar{\Psi}_i \Psi_i \rangle)$ is the diagonal mass matrix, and $E = \langle b\alpha_s / (32\pi) G^2 \rangle$ with $b = 11N_c/3 - 2N_f/3$. Once the θ parameter in Eq.(2.10) is specified, there are no free parameters remaining. Everything is fixed in terms of the vacuum condensates: the chiral condensate is given by $\langle \bar{\Psi}_i \Psi_i \rangle = -(240 \text{ MeV})^3$ and E is given in terms of the gluon condensate by $E = \langle b\alpha_s / (32\pi) G^2 \rangle \simeq 0.003 \text{ GeV}^4$. The summation over all branches, parameterized by l , is the main difference between this effective Lagrangian and the VVW effective potential. This potential also possesses cusp singularities at certain values of the fields, which is a result of the quantization of the topological charge from the beginning. This type of piecewise potential is also present in certain supersymmetric theories [26].

Considering only small values of $(\theta - i \log \text{Det}U)$ in the thermodynamic limit ($V \rightarrow \infty$), the $l = 0$ branch dominates and the potential takes the following form:

$$V(U, \theta) = -E \cos \left[\frac{1}{N_c} (\theta - i \log \text{Det}U) \right] - \frac{1}{2} \text{Tr}(MU + M^\dagger U^\dagger). \quad (2.11)$$

We are free to choose a diagonal basis where $U = \text{diag}(\exp i\phi_q)$ with $q = u, d, s$. Once this is done, the potential in terms of the ϕ_i 's is:

$$V(\theta, \phi_i) = -E \cos \left(\frac{\theta - \sum \phi_i}{N_c} \right) - \sum_{i=1}^{N_f} M_i \cos \phi_i, \quad (2.12)$$

where M_i are the diagonal entries of the quark mass matrix which was introduced above. Notice that in Eq.(2.12), the θ parameter appears only in the combination $\sum \phi_i - \theta$. In order to study the θ dependence on the vacuum energy, we must minimize the potential and solve the following equation:

$$\sin \left(\frac{\theta - \sum \phi_i}{N_c} \right) = \frac{N_c M_i}{E} \sin \phi_i. \quad (2.13)$$

In the case where we have an $SU(N_f)$ isospin symmetry and $M_i \ll E$, the approximate solution is given by $\phi_i \sim \frac{\theta}{N_f}$. Making this substitution, the vacuum energy density as a function of θ is given as:

$$E_{vac}(\theta) = -E + m_q N_f \langle \bar{\psi} \psi \rangle \cos\left(\frac{\theta}{N_f}\right) + \mathcal{O}(m_q^2). \quad (2.14)$$

In addition to Eq.(2.14), one can also calculate the topological charge density $Q = \langle 0 | \frac{\alpha_s}{8\pi} G\tilde{G} | 0 \rangle$ as a function of θ :

$$\langle \theta | \frac{\alpha_s}{8\pi} G\tilde{G} | \theta \rangle = -\frac{\partial E_{vac}}{\partial \theta} = -m_q |\langle \bar{\psi} \psi \rangle| \sin\left(\frac{\theta}{N_f}\right). \quad (2.15)$$

The effective potential shown above in Eq.(2.10) represents the anomalous effective Lagrangian for QCD realizing broken conformal and chiral symmetries. The following three points reinforce this statement:

1. Eq.(2.11) correctly reproduces the Di Vecchia-Veneziano-Witten effective chiral Lagrangian ([13, 14]) in the large N_c limit. As was already mentioned, in the thermodynamic limit for small values of $(\theta - i \log \text{Det}U) < \pi$, the $l = 0$ branch dominates. Expanding this branch in powers of $1/N_c$, we arrive at the following:

$$V(U, \theta) = -E + \frac{E}{2N_c^2} (\theta - i \log \text{Det}U)^2 - \frac{1}{2} \text{Tr}(MU + M^\dagger U^\dagger) + \dots \quad (2.16)$$

which is identical to the VVW potential (Eq.(2.7)) except for the shift by the constant E . We see that the constant a in Eq.(2.7) just corresponds to $\frac{E}{N_c^2}$ in the above expansion. It turns out that this can be identified with a quantity called the topological susceptibility in pure Yang-Mills gauge theory.

2. It reproduces the anomalous conformal and chiral Ward identities of QCD. If we consider the limit of $SU(N_f)$ isospin symmetry with $N_f = 3$ flavors of light quarks

($m_q \ll \Lambda_{QCD}$), the anomalous Ward identity given in [27, 28] can be obtained if we then differentiate Eq.(2.14) twice with respect to θ :

$$\begin{aligned} \lim_{q \rightarrow \infty} i \int dx \langle 0 | T \left(\frac{\alpha_s}{8\pi} GG(x) \frac{\alpha_s}{8\pi} GG(0) \right) | 0 \rangle &= -\frac{\partial^2 E_{vac}(\theta)}{\partial \theta^2} \\ &\simeq \frac{m_q}{N_f} \langle \bar{\psi} \psi \rangle + \mathcal{O}(m_q^2), \end{aligned} \quad (2.17)$$

in the approximation where θ is small. The other Ward identities can also be reproduced in a similar fashion from Eq.(2.10).

3. It reproduces the known dependence in θ (*ie.* 2π periodicity of observables) [13, 14]. If one examines the θ -dependence of the potential given in Eq.(2.11), the naive claim would be that the 2π periodicity desired for physical observables is absent and instead it is periodic in θ/N_c . This is not true as Eq.(2.11) represents only one particular vacuum state, $l = 0$. If we consider the sum over all vacuum states as in Eq.(2.10), we see that θ and $\theta + 2\pi$ are physically equivalent states and there is actually no problem at all.

We will now proceed and use Eq.(2.12) as a model for the creation of an induced θ -state in heavy ion collisions. It should be noted that the following analysis is independent of the exact form of the potential and in principle one could choose the VVW potential in place of the HZ potential which was just presented.

Chapter 3

Induced Theta Vacua

The long awaited Relativistic Heavy Ion Collider (RHIC) at Brookhaven National Laboratory could yield many fascinating results concerning the accepted theory of the strong force, QCD. Although the main goal of this experiment is to study the quark-gluon plasma, there exists many other possibilities. One of the most sought after results is the nature of the chiral symmetry restoration and/or deconfining phase transition. Another possible outcome is the so called disoriented chiral condensate (DCC). In the following chapter we will provide evidence that it may be possible to create an induced $\theta \neq 0$ -state in heavy ion collisions. If this is possible, the consequences could include the observation of a new form of matter where the physics is quite different from what is familiar to us.

In the following chapter, we use the low energy effective Lagrangian to show that a non-trivial θ^{ind} -vacua can be created in heavy ion collisions. Our calculations will follow closely the ideas presented in discussing the formation of a disoriented chiral condensate. Through the use of a simplified numerical model based on the Lagrangian presented in Section 2.3 we will estimate the time it takes for a non-trivial θ^{ind} -state to form. Despite of the fact that our calculations are based on a simplified model which differ somewhat from the real physics associated with high energy collisions, there is no reason to believe that a θ^{ind} -state cannot be created at RHIC. If the θ^{ind} -state can be experimentally detected, it must form within the time that the central region of the fireball (quark-gluon plasma) is isolated from the true vacuum.

3.1 What is the difference between θ^{ind} and the fundamental θ parameter?

The idea of an induced θ -state is very similar to the creation of the Disoriented Chiral Condensate (DCC) in heavy ion collisions [17, 18, 19, 20, 21] (see [29] for a discussion of DCC as an example of an out of equilibrium phase transition). DCC refers to regions of space (interior) in which the chiral condensate points in a different direction from that of the ground state (exterior), and separated from the latter by a hot shell of debris. For both cases (DCC and θ^{ind} -state) the difference in energy between a created state and the lowest energy state is proportional to the small parameter m_q and negligible at high temperature (see Eq.(3.3) below). This is necessary as it was previously believed that the creation of a θ^{ind} -state would be associated with the larger constant E .

We would like to stress the point that an induced θ -parameter is very different from θ^{fund} which is zero in our world and which cannot be changed. Above the temperature T_c at which the QCD phase transition occurs, the quark phases ϕ_i may be, in general, arbitrary. Given this, the singlet term $\phi_{singlet} = \sum \phi_i$, which is related to the η' , is non-zero. This can be identified with θ^{ind} -state as it can be rotated away by performing a $U(1)_A$ rotation of the fundamental QCD Lagrangian, at the cost of introducing an induced θ term in Eq.(2.12), $\theta^{ind} = -N_f \phi_{singlet}$. This non-vanishing singlet term could also be referred to as a zero (spatially constant) mode of the η' field. Since the symbol η' is usually associated with the excitation of the η' -field corresponding to the η' -meson and not with a classical constant field (condensate) configuration, we will refer to it as a θ^{ind} -state as we are free to perform a $U(1)_A$ rotation. Although the fundamental θ -parameter remains zero, we would expect that an induced θ -parameter will mimic the physics of the world with $\theta^{fund} \neq 0$. From now on we will refer to a θ^{ind} -state as simply a θ -state, thus omitting the “ind” label.

3.2 Disoriented Chiral Condensate

We will now describe the disoriented chiral condensate scenario as given in [17] to emphasize the similarities between the DCC and the θ -vacuum state. Rajagopal and Wilczek [17] use the $O(4)$ linear sigma model (see Sect. 2.1) to describe the low energy dynamics of the pions and the chiral condensate. All fields are represented by a 4-vector with components $\phi = (\sigma, \vec{\pi})$, where σ represents the chiral condensate and $\vec{\pi}$ represents the triplet of pions. Throughout the exterior region the vacuum expectation value of ϕ is $(v, 0)$. In the interior region, however, the pion fields can become non-zero and $(\sigma, \vec{\pi})$ wanders in the four dimensional configuration space. The high energy products (shell of debris) of the collision expand outwards at relativistic speeds and separates the misaligned vacuum interior from the exterior region.

In [17], all calculations were done under the assumption of a quenched system. In the quenched approximation, the $(\sigma, \vec{\pi})$ fields are suddenly removed from a heat bath ($T \geq T_c \sim 150 \text{ MeV}$) and evolved according to zero temperature Lagrangian dynamics. This is done numerically by giving the fields a non-zero vacuum expectation value $\langle \phi \rangle \neq 0$ and letting this field configuration evolve in time according to the zero temperature equations of motion. There is no reason to ignore the possibility that regions of misaligned vacuum with an arbitrary isospin direction will be created. In [17], it was shown that if the process is very rapid and the system is out of equilibrium, there is a temporary growth of long wavelength spatial modes of the pion field corresponding to domains where the chiral condensate is approximately correlated. In the case of DCC, the created state will relax to the true vacuum by coherent emission of pions with the same isospin orientation producing clusters of charged or neutral pions. DCC has been suggested as a possible explanation of certain events reported in the cosmic ray literature called Centauro and anti-Centauro events.

Let us consider the case $N_f = 2$. The matrix U is parameterized by the misalignment angle ϕ and the unit vector \vec{n} in the isospin space:

$$U = e^{i\phi(\vec{n}\vec{\tau})}, UU^\dagger = 1, \langle \bar{\Psi}_L^i \Psi_R^j \rangle = -|\langle \bar{\Psi}_L \Psi_R \rangle| U_{ij}.$$

The energy density of the DCC is determined by the mass term:

$$E_\phi = -\frac{1}{2} \text{Tr}(MU + M^\dagger U^\dagger) = -2m|\langle \bar{\Psi}\Psi \rangle| \cos(\phi), \quad (3.1)$$

Eq. (3.1) implies that any $\phi \neq 0$ is not a stable vacuum state because $\frac{dE}{d\phi} \neq 0$, *ie.* the vacuum is misaligned. Since the energy difference between the misaligned state and the true vacuum is proportional to m_q , the probability to create a state with an arbitrary ϕ at high temperature $T \sim T_c$ is proportional to $\exp[V(E_\theta - E_0)/T]$ and depends on ϕ only very weakly. In other words ϕ is a quasi-flat direction. Right after the phase transition when $\langle \bar{\Psi}\Psi \rangle$ becomes non-zero, the pion field oscillates. The coherent oscillations of the π -meson field would correspond to a zero-momentum condensate of pions. Eventually these classical oscillations produce real π -mesons which can hopefully be observed.

3.3 θ -State in Heavy Ion Collisions

As we discussed in Sect. 3.1, the formation of the θ -vacuum state could occur when the $U(1)_A$ phase of the chiral condensate is in general non-zero. The difference between the formation of θ -vacua and DCC is twofold:

- (i) In addition to chiral fields differing from their true vacuum expectation values the θ -parameter of QCD, which is zero in the real world, becomes effectively non-vanishing in the interior of the shell of debris.
- (ii) The disoriented chiral condensate involves the amplification of the charged pions while the formation of the θ -vacuum state involves the amplification of the low momentum modes of only the neutral particles. This includes the η' singlet as we shall see below.

We will choose a diagonal basis for the matrix U_{ij} in order to take into account the $U(1)_A$ phase associated with θ -vacua. The energy density of the misaligned vacuum is determined in this case by the potential given by Eq.(2.12) and derived in [1, 2]:

$$V(\theta, \phi_i) = -E \cos\left(\frac{\theta - \sum \phi_i}{N_c}\right) - \sum_{i=1}^{N_f} M_i \cos \phi_i, \quad (3.2)$$

where $E = \langle b\alpha_s/(32\pi)G^2 \rangle \sim 10^{-2} \text{ GeV}^4$ is much larger than $M_i = -m_q \langle \bar{\Psi}\Psi \rangle \sim 10^{-3} \text{ GeV}^4$. The fact that the θ -parameter appears only in the combination $\sum \phi_i - \theta$ is very important for the formation of a θ -state. If we consider the limit where all the quark masses are equal and $M_i \ll E$, the approximate minimum of this potential is given by $\phi_i \sim \frac{\theta}{N_f}$. In this case, the difference in the vacuum energy when $\theta = 0$ and $\theta \neq 0$ for $N_f = 2$ is given by:

$$V_{vac}(\theta) - V_{vac}(\theta = 0) \simeq -2m_q |\langle \bar{\psi}\psi \rangle| \left(\left| \cos \frac{\theta}{2} \right| - 1 \right). \quad (3.3)$$

From this we see that the cost of creating a non-trivial θ -state goes like the much smaller parameter $m_q \langle \bar{\Psi}\Psi \rangle$ and that a θ -state is degenerate with the $\theta = 0$ -state in the chiral limit where $m_q = 0$, as expected. The combination $\sum \phi_i - \theta$ is a direct consequence of the transformation properties of the chiral fields under a $U(1)_A$ rotations.

If we compare Eqs. (3.1) and (3.2), we see that in Eq. (3.2) there is a large term $\sim E \gg m_q |\langle \bar{\Psi}\Psi \rangle|$. In the chiral limit, this term does not vanish and provides a non-zero mass for the η' -meson which is expressed in terms of the parameter, E . Since θ is associated with the large parameter E , it is often assumed that the creation of non-trivial θ -vacua would involve too large an energy cost. It was pointed out in [30] that this is not necessarily the case.

The crucial point arises when one considers the scenario suggested for DCC where the chiral phases ϕ_i acquire random values, the energy of a misaligned state differs by a large amount proportional to E from the vacuum energy. In order to produce long

wavelength oscillations (a macroscopically correlated region)¹, the potential must have a quasi-flat ($\sim m_q$) directions along the ϕ_i coordinates. This is not the case if the misaligned state differs from the vacuum state by an amount $\sim E$. However, when the relevant combination ($\sum_i \phi_i - \theta$) from Eq.(3.2) is close by an amount $\sim \mathcal{O}(m_q)$ to its vacuum value, a Boltzmann suppression due to the term $\sim E$ is absent, and an arbitrary misaligned θ -state can be formed.

In order to study the time evolution of the chiral phases numerically, several assumptions must be made. First, assume that the θ -parameter acquires a non-zero value on a macroscopically large domain when the temperature $T \gg m_q$ and the system is out-of-equilibrium. Once again, $\theta \neq 0$ follows from the assumption that the singlet phases $\langle \sum \phi_i \rangle \neq 0$ immediately upon cooling through the phase transition. Performing a $U(1)_A$ rotation then gives us $\theta \neq 0$. The second assumption is that the phases ϕ_u , ϕ_d , and ϕ_s have small random values at these high temperatures. Third, the rapid expansion of the high energy shell leaves behind an effectively zero temperature region in the interior which is isolated from the true vacuum. The high temperature non-equilibrium evolution is very suddenly stopped, or “quenched”, leaving the interior region in a non-equilibrium initial state that then begins to evolve according to zero temperature Lagrangian dynamics. Starting from an initial non-equilibrium state we can study the behavior of the chiral fields using the zero temperature equations of motion. The equations of motions are non-linear and cannot be solved analytically but we can solve them numerically in order to determine the behavior of the fields. Finally, by realizing that the chiral fields relax to a constant, equal, and non-zero values on a time scale over which spatial oscillations of the fields vanish (*ie.* only the zero momentum mode remains), we show that a θ -state has been formed. The formation of a nonperturbative condensate is also

¹In referring to a macroscopically large domain, the region considered to be macroscopic compared to the scale of the system, Λ_{QCD}^{-1} .

supported by observation of the phenomenon of coarsening (see below) and by a test of volume-independence of our results.

3.4 Evolution of the Equations of Motion

We will now present the results obtained from the numerical evolution of the chiral fields on a cubic lattice. The equations of motion for the phases of the chiral condensate with two quark flavors consists of two coupled second order nonlinear partial differential equations:

$$\ddot{\phi}_i - \nabla^2 \phi_i + \gamma \dot{\phi}_i + \frac{d}{d\phi_i} V(\phi_1, \phi_2, \theta) = 0, \quad i = 1, 2, \quad (3.4)$$

where ∇^2 is a three dimensional spatial Laplacian and the potential is given in Eq. (3.2). There is obviously some sort of damping present in any real system, and this damping can be attributed to the expansion of the region inside the shell (dilution of energy) and/or the radiation of Goldstone bosons. The damping constant, γ , was chosen to be of the same order of magnitude as $\Lambda_{QCD} \sim 200 \text{ MeV}$, which should be a reasonable value according to all other scales present in the system.

The initial data for each of the chiral fields ϕ_i is placed on a $3 - d$ grid of 16^3 points, with ϕ_i chosen from a uniform distribution and $\dot{\phi}_i = 0$. The initial data was evolved in time using a Two-Step Adams-Bashforth-Moulton Predictor-Corrector method for each grid point with the spatial Laplacian approximated at each grid point using a finite difference method. We used periodic spatial boundary conditions.

The lattice spacing was set according to the the length of the side of the spatial grid, which was varied in order to vary the volume. We evolved the data for 8000 time steps of about 10^{-5} MeV^{-1} , which was much smaller than the lattice spacing. In order to examine the momentum dependence, we applied a Fast Fourier Transform [31] to the spatial data at evenly spaced time steps. The data was then binned in small increments

of the magnitude of the wave vector $|\vec{k}|$ in order to obtain the angular averaged power spectrum. The bin width was chosen to be as small as possible without resulting in some intervals being left empty.

The numerical simulation was carried out for different initial conditions and different volumes, with the results being qualitatively the same. Once the chiral phases ϕ_i were given random values, they begin to approach the true solution $\bar{\phi}_i \approx \theta/N_f$ and of course overshoot it. We saw an initial growth of long wavelength modes as in [17] and subsequent damped oscillation of all modes. The $|\vec{k}| = 0$ modes oscillated and approached the equilibrium values of the fields ($\phi_i \sim \theta/N_f$). All of the modes with $|\vec{k}| \neq 0$ decayed to zero before the $|\vec{k}| = 0$ mode reached the vacuum expectation value ($\phi_i \sim \theta/N_f$). The fact that this behaviour manifests itself for different total volumes and grid sizes suggests that our results are not due to finite size effects. Since we are working in a finite box with periodic boundary conditions, our $|\vec{k}| = 0$ mode is really only a quazero mode. However, our quazero mode approaches the same value irrespective of the total spatial volume indicating that this really is a condensate. If it were not we would expect the value of the coefficient to decrease when the volume of the system increases (as $\Delta k \sim 1/\Delta x$).

The evolution of the Fourier modes of the ϕ_i fields as a function of time is shown in Fig. 3.1 for the specific case of $\theta = 2\pi/16$ and a spatial volume of $(10 fm)^3$. We assigned each of the fields an equal mass of about $5 MeV$. The initial values of the chiral phases were chosen randomly, with $|\phi_i| < 7\pi/16$ and $\dot{\phi}_i = 0$. In Fig. 3.1, we show the zero mode and three of the higher momentum modes. It is obvious that the zero mode settles down to a non-zero value $\sim \theta/N_f$ while all higher modes vanish extremely rapidly and are negligible long before the zero mode settles down to its equilibrium value.

We have also examined ϕ_i as a function of $|\vec{k}|$ for different times. The instantaneous distribution of Fourier modes for the evolution above is shown in Fig. 3.2 at a few

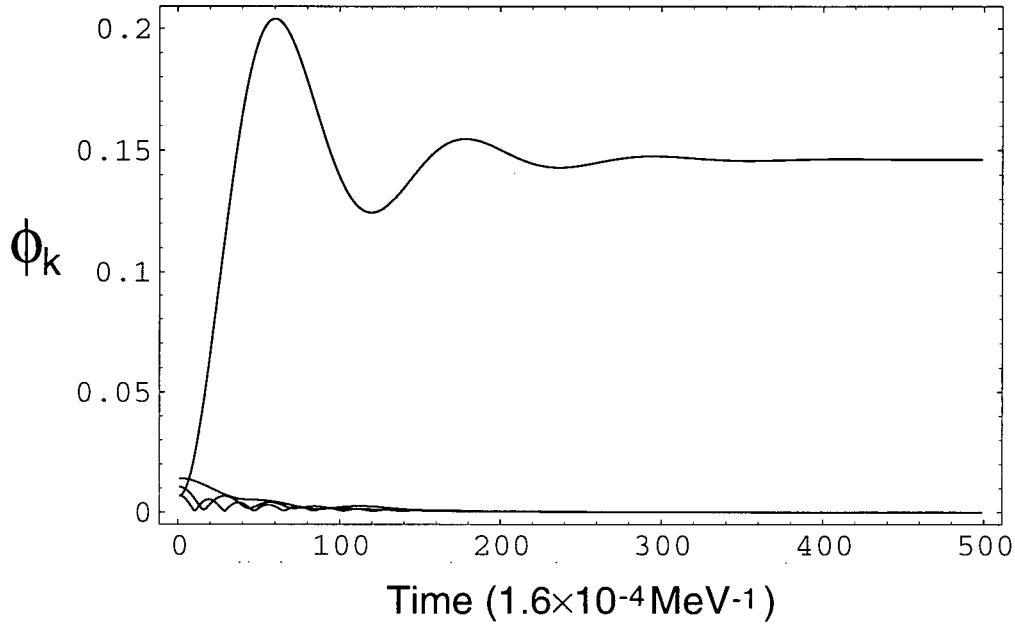


Figure 3.1: $|\phi_k|$ is shown for various $|\vec{k}|$ as a function of time. In a time $\sim 10^{-23}$ sec, the zero mode relaxes to $\bar{\phi}_i \sim \theta/N_f$ and all other modes decay to zero. This is very similar to the idea of a disoriented chiral condensate.

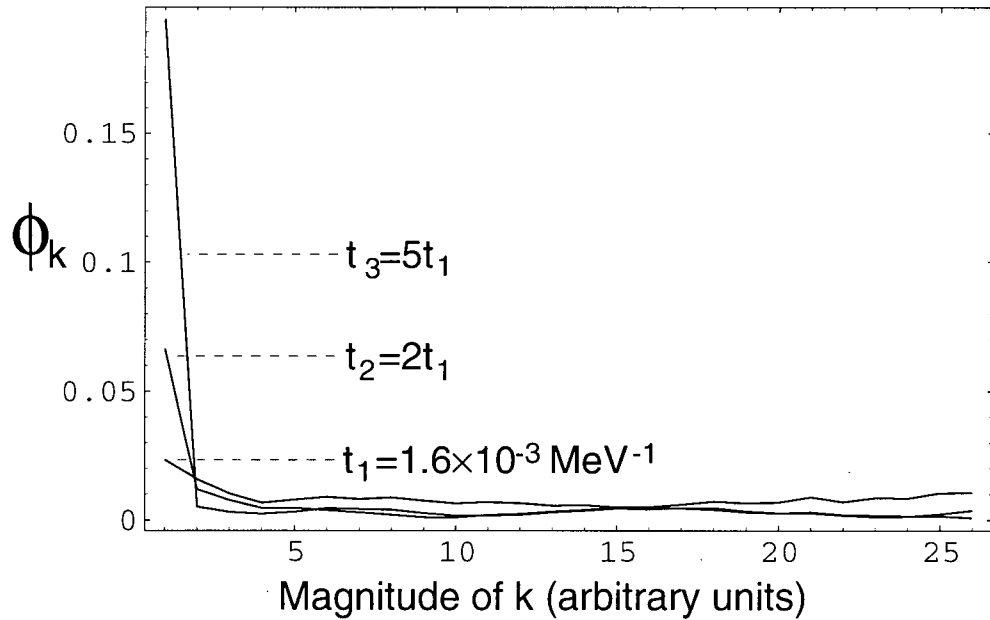


Figure 3.2: Above we demonstrate that the system exhibits the coarsening phenomenon (amplification of the zero mode as time increases). The data was sampled at three times within the first 1000 time steps of the evolution.

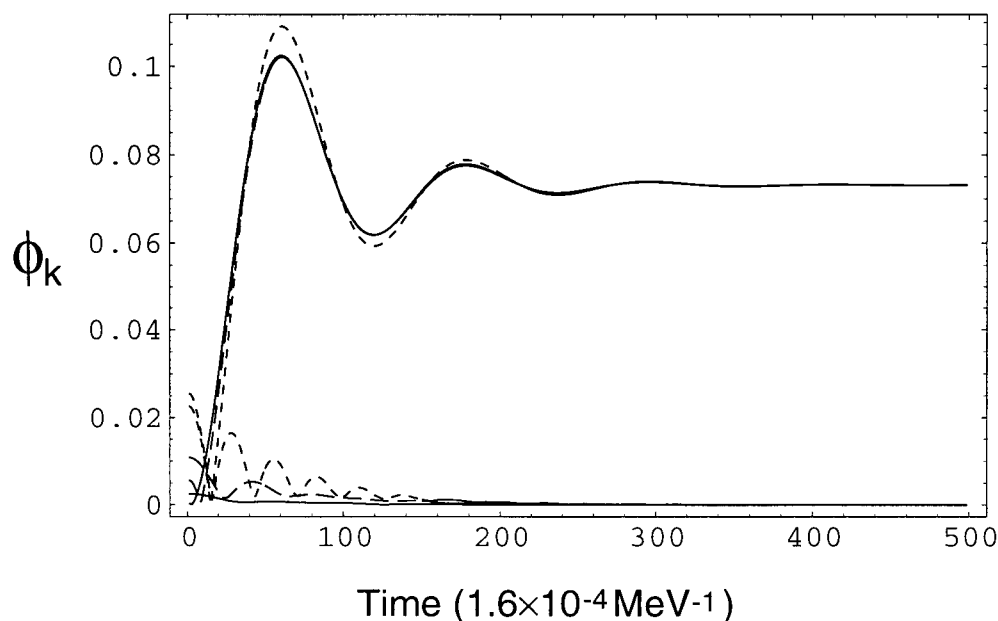


Figure 3.3: The zero mode and a non-zero mode are shown as a function of time for three different volumes. The heavily dashed line represents the smallest volume $(8 \text{ fm})^3$, the medium dashed line represents the middle volume $(16 \text{ fm})^3$, and the solid line represents the largest volume $(32 \text{ fm})^3$. The volume independence of the zero mode reinforces the claim that a true nonperturbative condensate has been formed.

different times. This graph clearly demonstrates the phenomenon of coarsening, which is the amplification of the zero mode with increasing time. Coarsening and the formation of a nonperturbative condensate is discussed in greater detail in [29].

In Fig. 3.3 we plot $|\phi_k|$ as a function of time for three different volumes. We chose $\theta = \pi/16$ and the volumes $(8 \text{ fm})^3$, $(16 \text{ fm})^3$, and $(32 \text{ fm})^3$. We plotted the zero mode and one of the higher momentum modes for each volume. Notice that the zero mode is independent of the volume of the system, while the magnitude of the non-zero mode decreases with increasing volume. This is the signature that a real nonperturbative condensate has been formed.

For a total volume of $(10 \text{ fm})^3$ and $\theta = 2\pi/16$ the time for relaxation from the initial nonequilibrium state following the quench to the non-trivial θ -vacuum is approximately

$0.064 \text{ MeV}^{-1} \approx 4 \times 10^{-23} \text{ s}$. The central region of the fireball is estimated to be isolated from the true vacuum ($\theta = 0$) for a time $\tau_{\text{fireball}} \sim 10 \text{ fm}/c \sim 10^{-23} \text{ s}$. Given this estimate for τ_{fireball} , we see that the formation of a θ -state is of the same order of magnitude. The volume we have used is just at the upper limit of what we would expect at RHIC for the transverse direction. In spite of the fact that we have not taken into account the correct physical collision geometry, our simplified calculation suggests the possibility of producing non-trivial θ -vacua.

In the preceding sections, we have shown that the realization of an induced θ -state may be possible in heavy ion collisions. Through the use of a numerical simulation of the zero temperature equations of motion, we have shown that the chiral fields ϕ_i go to a spatially constant non-zero value related to the θ -parameter ($\phi_i \sim \theta/N_f$) in a time of about 10^{-23} s . All simulations relied upon the quenched approximation where we assume that the system is suddenly removed from a high temperature heat bath $\sim T_c$ and subsequently evolved according to the zero temperature equations of motion. The following two facts confirm that the a true nonperturbative condensate (θ -vacuum state) has been formed: (i) All non-zero modes decay to negligible values long before the zero mode reaches its equilibrium value, (ii) The zero mode is independent of the volume of the system while the non-zero modes decrease with increasing volume.

Chapter 4

Signatures of an Induced θ -Vacuum State

One might ask, “How could such a θ -state be detected if it is created in heavy ion collisions?” If the correlation length of the created region is large and the system is in thermal equilibrium, axions would be the obvious thing to look for. If we assume the existence of axions, they should in principle be produced upon relaxation of the $\theta^{ind} \neq 0$ to the lower energy state with $\theta = 0$. However, since it is unlikely that the system will be in thermal equilibrium and the size of the created region is not expected to be very large ($\approx (10 \text{ fm})^3$) axion production does not look very promising if we compare to the limit already achieved from astrophysical and cosmological considerations [7, 8, 9]. This forces us to look to must other possibilities. Another possibility is that the θ -state could be observed through Goldstone bosons with specific P , CP -odd correlations [32, 33]. This possibility must be considered due to the non-zero value for the topological charge density with $\theta \neq 0$ in Eq.(2.15). It was recently pointed out [24] that this effect would probably be washed out due to the rescattering of pions and their interactions in the final states, which mimic true CP -odd effects.

As was shown in Chapter 3, the creation of the θ -vacuum state involves the enhancement of the low momentum modes of the chiral fields. Considering this, we should look for enhanced production of particles such as the π^0 , η , and η' -mesons with low momentum, on the $(10 - 100) \text{ MeV}$ scale (depending on the size of the domain L). These should decay by various processes to photons and dileptons, and if it is possible to detect a large number of these low momentum particles this would be a definite signal of the creation

of a θ -state. In the following we will provide further evidence that this is the case and could also account for the unexplained large number of low momentum dileptons seen at CERN [3, 4]. This idea was originally proposed in [24]. In order to support this speculative conjecture more in depth calculations must be performed.

4.1 Properties of the pseudo-Goldstone Bosons in the non-zero θ -Background

As was shown in [23, 24], the properties of the pseudo-Goldstone¹ bosons are altered in the presence of a non-zero θ -background. This has been suggested as a possible signature of the formation of a non-trivial θ -state. In the θ -world, the masses of the octet of Goldstone bosons and the η' singlet are decreased. For instance, a calculation of the mass matrix for an arbitrary value of θ with $m_u = m_d = m_q$ gives [23, 24]:

$$\begin{aligned} m_\pi^2 &= \frac{4}{f_\pi^2} M_q \left| \cos \frac{\theta}{2} \right|, \\ m_\eta^2 &= \frac{4}{3f_\pi^2} (2M_q \left| \cos \frac{\theta}{2} \right| + 2M_s), \\ m_{\eta'}^2 &= 4 \frac{EN_f}{f_\pi^2 N_c^2} + \frac{4}{N_f} \frac{1}{f_\pi^2} (2M_q \left| \cos \frac{\theta}{2} \right| + M_s). \end{aligned} \quad (4.1)$$

As well, these particles become a mixture of pseudoscalar/scalar rather than pure pseudoscalars as for $\theta = 0$. The mixing angle between the singlet and octet combinations depends on the θ -parameter [23]. This fact means that the CP -odd decays $\eta \rightarrow \pi\pi$ and $\eta' \rightarrow \pi\pi$ are no longer suppressed in the θ -background and become of order 1 [24]. These matrix elements were recently calculated [24] to give the following results:

$$\begin{aligned} \Gamma(\eta \rightarrow \pi\pi) &= \frac{2 \left(1 - \frac{4m_\pi^2(\theta)}{m_\eta^2(\theta)} \right)^{\frac{1}{2}}}{3\pi m_\eta(\theta)} \left(\frac{m_q \sin \frac{\theta}{2} \langle 0 | \bar{q}q | 0 \rangle}{f_\pi^3} \right)^2, \\ &\sim 0.5 \text{MeV} \left(\sin \frac{\theta}{2} \right)^2, \end{aligned} \quad (4.2)$$

¹From now on the pseudo-Goldstone bosons will be referred to as simply Goldstone bosons.

$$\begin{aligned}\Gamma(\eta' \rightarrow \pi\pi) &\sim \frac{6}{\pi m_{\eta'}} \left(\frac{m_q \sin \frac{\theta}{2} \langle 0 | \bar{q}q | 0 \rangle}{f_\pi^3} \right)^2, \\ &\sim 2 \text{ MeV} \left(\sin \frac{\theta}{2} \right)^2.\end{aligned}\tag{4.3}$$

The full width of the η', η decays in our world are much larger than the above decays in the θ -world. The particle data booklet gives $\Gamma^{total}(\eta) \sim 118 \text{ keV}$ and $\Gamma_{\theta=0}^{total}(\eta') \sim 0.2 \text{ MeV}$ as the full experimental widths. Therefore, the widths could be increased by as much as an order of magnitude in the θ -world.

Thus observation of an increased rate of decay of η', η at masses slightly shifted from the accepted values would be a signature of the θ -vacuum. However, this signal may be a difficult one to distinguish in the large amounts of data generated in a heavy ion collisions. Therefore we would like to discuss a signature that would be easier to observe experimentally.

4.2 Signature of the Creation of θ -Vacua

In this section we consider an additional new signature which could possibly verify if a θ -state can be created in heavy ion collisions. As was discussed briefly in the introduction, the creation of a θ -state could greatly enhance the production of low momentum ($\sim 25 \text{ MeV}$) Goldstone bosons.

Before going into the details we would like to discuss the concepts behind this idea. We have already presented evidence that a θ -state can be formed in heavy ion collisions if protected from the exterior $\theta = 0$ world by the shell of debris. At some point, however, this shell ceases to isolate the interior and the influence of the exterior world will be felt. The way in which this happens is not well understood, but we would like to use an instantaneous approximation in order to obtain some approximate results. There are basically two time scales present in the system: the lifetime τ_{shell} of the shell separating

the two worlds and the scale associated with strongly interacting particles, $(\Lambda_{QCD})^{-1}$. If these differ by orders of magnitude, the disappearance of the shell can be considered either as an instantaneous perturbation or an adiabatic perturbation.

Realistically, we expect τ_{shell} to be about the same order of magnitude as $(\Lambda_{QCD})^{-1}$ and therefore the disappearance of the shell is somewhere between an instantaneous process and an adiabatic one. However, we do not yet know how to treat the process properly so we will use the instantaneous approximation in order to obtain an order of magnitude estimate of the spectrum of emitted particles.

The instantaneous perturbation is an approximation that is well known in quantum mechanics. We assume that the shell separating the θ -vacuum state from the vacuum state with $\theta = 0$ instantaneously blows apart. Therefore, all states which had been formed in the induced θ -state will suddenly find themselves in a new vacuum state with $\theta = 0$. The θ^{ind} -states are now forced to transform to asymptotic states of our world with $\theta = 0$. We do not know how to treat this complex transformation exactly but if the process is instantaneous things simplify considerably and we can expand the initial state in terms of the asymptotic states of the $\theta = 0$ world.

The above approximation is applied to our calculation in the following way. The field values, ϕ_i , obtained for the θ -state in Chapter 3 is embedded into a larger grid where the field values take their $\theta = 0$ vacuum values. This data now contains a plateau of field values corresponding to θ -state values surrounded by zero field values. This field configuration must now resolve itself into asymptotic free particles. With this process in mind we determine the momentum spectrum of free particles corresponding to this distribution by considering the Goldstone boson fields as true quantum fields at this instant.

In order to calculate the spectrum, we must obtain the quantities $a(\vec{k})$ and $a^\dagger(\vec{k})$. These are obtained by performing the Fourier transform of the field configuration at

time $t = \tau_{shell}$ when the shell breaks down,

$$a(\vec{k}) = \int d^3\vec{x} \psi(\vec{x}) \exp(-i\vec{k} \cdot \vec{x}), \quad (4.4)$$

where $\psi(\vec{x})$ is the distribution amplitude of the ϕ_i fields obtained from evolving the equations of motion (Eq.(3.4)) on a cubic lattice, as was done in Chapter 3. From Eq.(4.4), the number operator is given by $N(\vec{k}) = N_o a(\vec{k}) a^\dagger(\vec{k})$ where N_o is an overall constant that will be determined using the following argument. As we mentioned earlier, the θ -vacuum state differs from the true vacuum state by a small amount of energy $\sim m_q$. The amount of energy that is available when the θ -vacua decays is obtained by analyzing the θ -dependence of the vacuum energy density E :

$$E_\theta = m_q |\langle \bar{\Psi} \Psi \rangle| N_f \cos\left(\frac{\theta}{N_f}\right). \quad (4.5)$$

Therefore, the amount of energy $\Delta\mathcal{E}$ available due to the formation of the θ -state is given by

$$\begin{aligned} \Delta\mathcal{E} &= (E_{\theta=0} - E_\theta) \cdot V \\ &= m_q |\langle \bar{\Psi} \Psi \rangle| N_f \left(1 - \cos\left(\frac{\theta}{N_f}\right)\right) \cdot V \\ &\approx 20 \left(\frac{V}{(10 \text{ fm})^3}\right) \text{ GeV}, \end{aligned} \quad (4.6)$$

where V is the the volume of the created θ -region. If we take for example a θ -state with volume $V = (8 \text{ fm})^3$ the amount of energy available is $\Delta\mathcal{E} = 10 \text{ GeV}$. This represents only a small amount of energy compared to cm energy, $\sqrt{s} = 40 \text{ TeV}$, expected in heavy ion collisions:

$$\rho \sim \frac{\Delta\mathcal{E}}{\sqrt{s}} \sim \frac{20 \left(\frac{V}{(10 \text{ fm})^3}\right) \text{ GeV}}{40 \text{ TeV}} \sim 10^{-3} \left(\frac{V}{(10 \text{ fm})^3}\right)$$

If the total amount of available energy is known, the constant N_o can be fixed by enforcing the following conservation of energy constraint:

$$\Delta\mathcal{E} = \sum_i \int \frac{d^3\vec{k}}{2(2\pi)^3} N_o a(\vec{k})_i a^\dagger(\vec{k})_i, \quad (4.7)$$

where the sum is performed over all types of particles considered (*ie.* all neutral Goldstone bosons). Once this constant N_o is fixed, the total number of pions and etas can be calculated by

$$N = \int \frac{d^3\vec{k}}{2\omega_k(2\pi)^3} N_o a(\vec{k}) a^\dagger(\vec{k}), \quad (4.8)$$

for the simplified case of only one collision of two gold nuclei. If we consider that RHIC will collide gold nuclei at a frequency of 1 kHz , we can estimate the total number of these low momentum particles produced by simple multiplication. All the results that follow are presented for just one event.

4.3 Results

As we have already mentioned, we proceed as follows. At some time t before the fields ϕ_i settle down to the constant field configuration (see Fig. 4.1), we take the position space data and embed this in a larger square grid where the field values are zero (our world). We assume an instantaneous perturbation and then take the Fourier transform of this field configuration in order to obtain the operators $a(\vec{k})$ and $a^\dagger(\vec{k})$. It may be argued that the instantaneous approximation is not valid in this case as we expect $\tau_{shell} \sim \tau_{QCD}$ and therefore this calculation gives us a rough estimate at best. In Fig. 4.1, we show at what point in the evolution of the ϕ_i fields we chose for τ_{shell} .

In order to calculate the spectrum of the diagonal (neutral) components of the matrix $U(\pi^0, \eta, \eta')$, we must make the following correspondence:

$$\begin{aligned} U &= \text{diag}(\exp i\phi_i) \\ &= \exp \left[i\sqrt{2} \frac{\pi^a \lambda^a}{f_\pi} + i \frac{2}{\sqrt{N_f}} \frac{\eta'}{f_{\eta'}} \right], \end{aligned} \quad (4.9)$$

to obtain the π_o , η , and η' in terms of the ϕ_i 's:

$$\pi^0 = \frac{f_\pi}{2\sqrt{2}} (\phi_u - \phi_d), \quad (4.10)$$

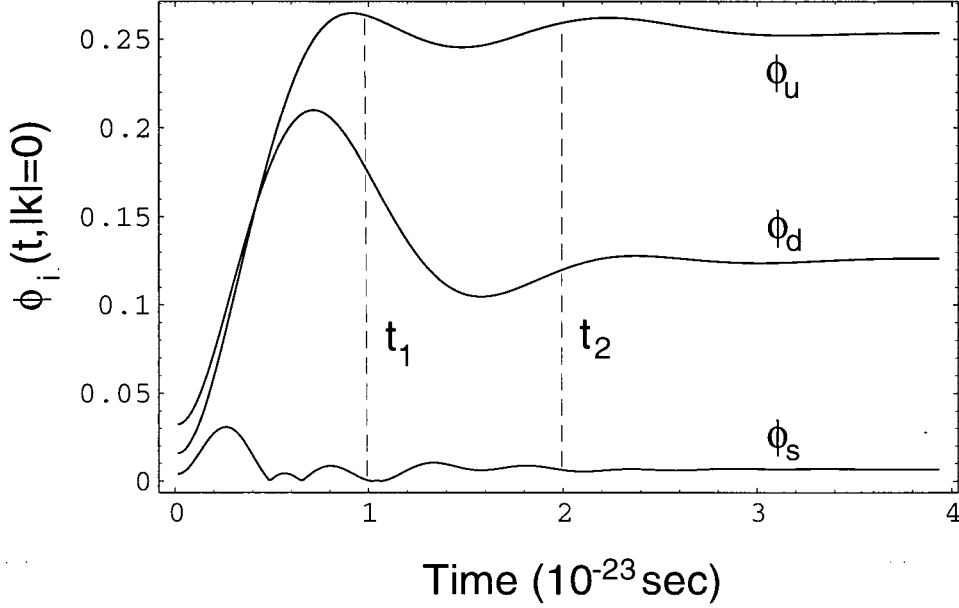


Figure 4.1: $|\phi_i(k=0)|$ is plotted as a function of time for the up, down, and strange quark. Notice that the zero momentum modes of the ϕ_i fields settle to a non-zero value in a time on the order of 10^{-23} s. The times t_1 and t_2 represent the value we chose for τ_{shell} , the time when the shell separating the two regions disappears.

$$\eta = \frac{f_\pi}{2\sqrt{6}}(\phi_u + \phi_d - 2\phi_s), \quad (4.11)$$

$$\eta' = \frac{f_{\eta'}}{2\sqrt{3}}(\phi_u + \phi_d + \phi_s). \quad (4.12)$$

For all numerical calculations, we can take the constant $f_{\eta'}$ to be $\sim f_\pi$. One of the crucial decisions which must be made is when to choose the time at which the shell breaks down. We chose several values for τ_{shell} . As τ_{shell} gets larger, the majority of the particles which are produced due to the formation of the $|\theta\rangle$ state have momentum $k < 25$ MeV. In Fig. 4.2, we show a plot of $N_{\pi^0}(k)$ as a function of $|\vec{k}|$ for the neutral pion. The function $N_{\pi^0}(k)$ has dimensions MeV^{-1} , so that the total number of particles, N_{π^0} , is a dimensionless number given by:

$$N_{\pi^0} = \int_{-\infty}^{\infty} dk N_{\pi^0}(k) = \int_{-\infty}^{\infty} dk \frac{4\pi}{2(2\pi)^3 \omega_k} N_o a(\vec{k}) a(\vec{k})^\dagger. \quad (4.13)$$

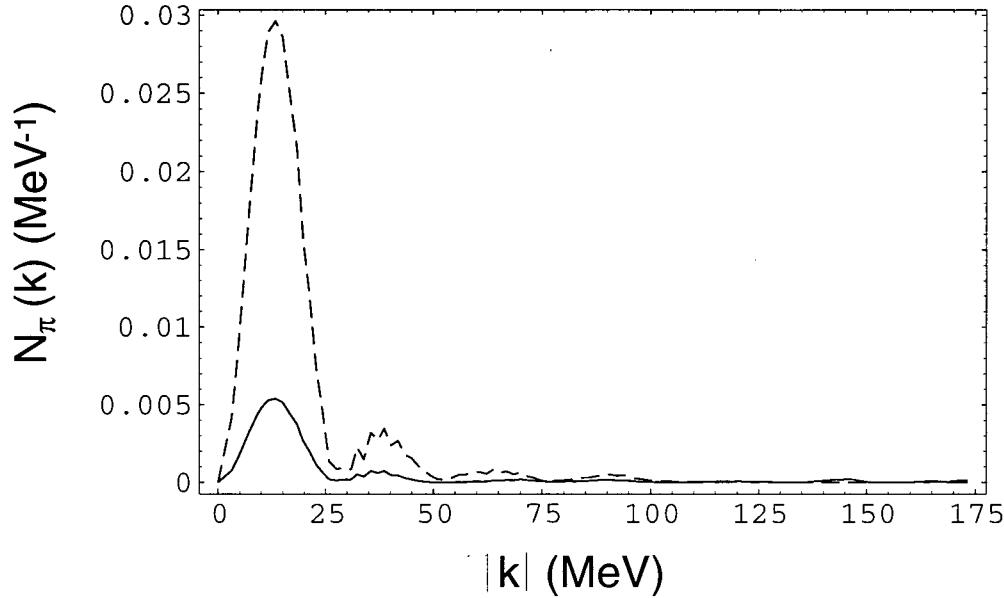


Figure 4.2: We plot the number of pions produced, $N_{\pi^0}(k)$ as a function of the magnitude of the wave vector, $|\vec{k}|$. Above we show that the momentum distribution of the π^0 -mesons produced is primarily $< 25 \text{ MeV}$ for two different values of τ_{shell} . The solid line represents the earlier time t_1 and the dotted line represents the later time t_2 (see Fig. 4.1 for the positions of t_1 and t_2 in the evolution of the ϕ_i fields). This is expected as the formation of the θ -state can be attributed to the enhancement of the low momentum modes.

The two different lines represent the times at which we assumed the shell to break down. The solid line represents the earlier time $\tau_{shell} = t_1 = 1500/6000$ time steps $\sim \frac{10^{-23}}{4} \text{ s}$ while the dotted line represents $\tau_{shell} = t_2 = 3000/6000$ time steps $\sim \frac{10^{-23}}{2} \text{ s}$ (this representation for t_1 and t_2 will be used in all graphs that follow). For this calculation, we assumed the created θ -state had a volume of $(8 \text{ fm})^3$ which exists in a larger volume of $(64 \text{ fm})^3$. The explanation of this phenomenon is simple: at time t_1 the amplification of the zero mode is not as large as at time t_2 . Furthermore, at time t_1 a considerable portion of the energy goes to high momentum particles.

We show the same graph for the η -meson and the η' -meson. Notice that that the η' is produced in copious amounts compared to the π^0 -mesons and the η -meson. In order to obtain the total number of each particle produced, we use Eq.(4.8) to calculate the

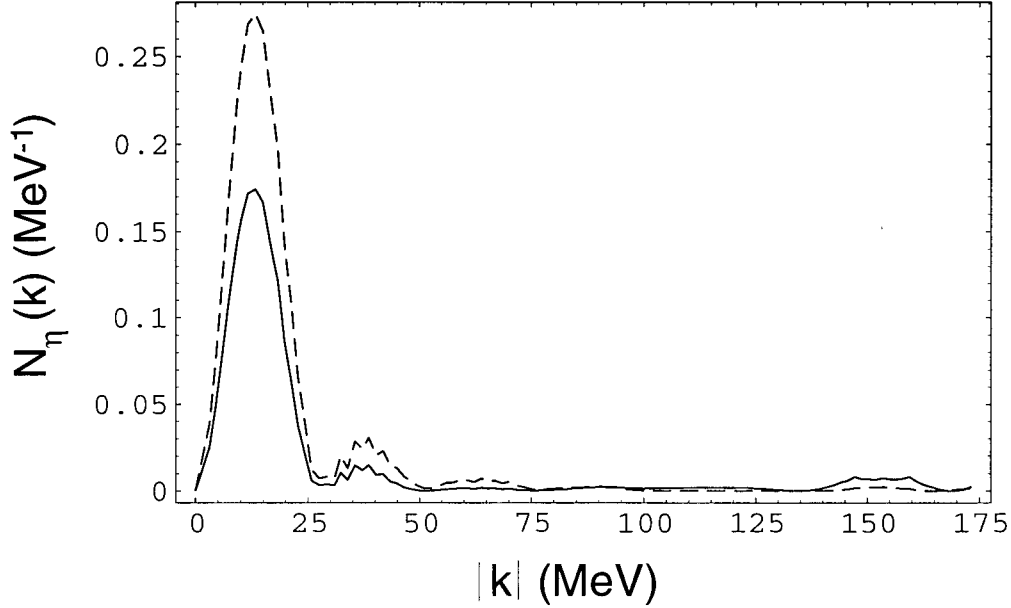


Figure 4.3: $N_\eta(K)$ is plotted as a function $|\vec{k}|$, at two different times t_1 and t_2 as in Fig. 4.2. The higher peak represents the later time with the main difference being that now a larger percentage of the produced particles lie in the $k < 25 \text{ MeV}$ range.

total number of particles produces per collision: $N_{\pi^0} = 0.1$, $N_\eta = 2.8$, $N_{\eta'} = 19.3$ for $t = t_1$ and $N_{\pi^0} = 0.5$, $N_\eta = 4.3$, $N_{\eta'} = 18.4$ for $t = t_2$. We have also checked that in the limit where all quark masses are equal, only the η' is produced, as expected. It should be noted that as demonstrated by these figures and the coarsening phenomenon (i.e. the phenomenon of amplification of the zero mode as time increases), we would expect that as τ_{shell} increases up to a maximum value, the majority of the particles would reside in the low momentum regime. We consider our analysis to be a lower bound on the number of produced particles due to the fact that we do not include the particles which would be produced during the formation of the θ -state. The particles that are produced during this period will have a higher momentum and therefore will be hard to detect in such the background of high momentum particles that is expected in heavy ion collisions. Our main conclusion is that the production of an induced θ -state will result in the emission

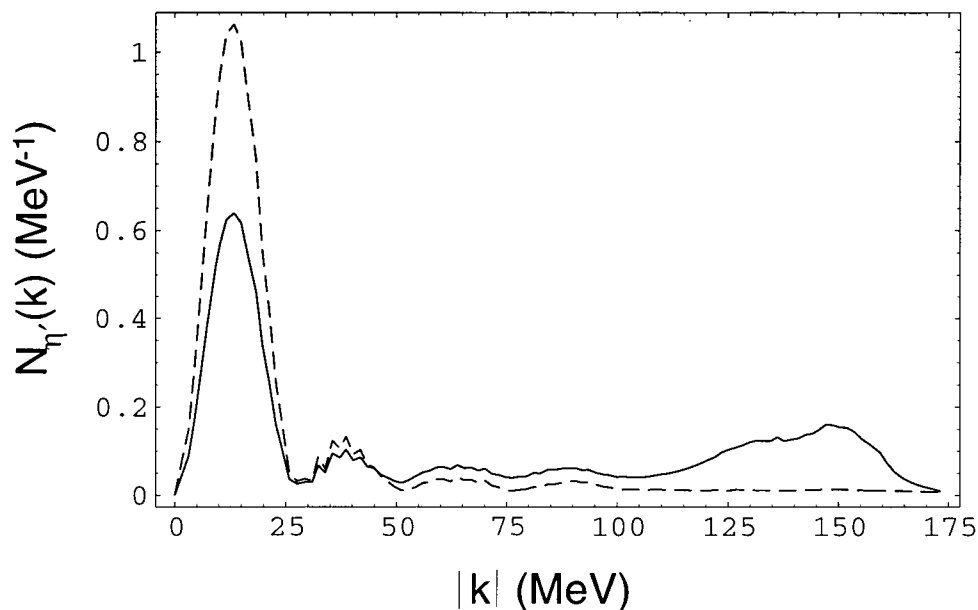


Figure 4.4: $N_{\eta'}(k)$ vs. $|\vec{k}|$ is shown above. This graph shows that the η' clearly dominates the spectrum compared to the other neutral particles.

of low-energy η and η' -mesons.

In a recent paper by Baier *et al.* [34], the production of an excess of η' -mesons is discussed in the scenario suggested in [32]. In [32] they use the VVW effective potential to show that upon cooling through the phase transition temperature T_c , metastable states may be formed where P and CP are violated. While the ideas presented in [34] are similar to the work presented in this paper, there are important differences to be noted. Our approach is essentially a two step process. First, we let the chiral fields evolve and observe that a non-trivial vacuum state has been formed. Once the θ -state has been realized, we assume that it instantaneously decays and calculate the particle production due to this single event, not taking into account previous particle production. We also assume a quenched system where the temperature changes quickly from $T \sim T_c$ to $T = 0$. Their approach is different from ours as their calculation of the number of produced η' -mesons receives contributions from all time, not just one particular instant. In order to calculate

the number of η' -mesons produced when the CP odd bubbles disappear in [34], they use the fact that at some temperature below the temperature T_c the metastable state disappears and becomes a saddle point. Once this saddle points forms the η' -field begins to roll down towards the true minima where CP is restored. The number of produced η' -mesons is calculated as a function of time by considering the quantum fluctuations about the vacuum expectation value of the field and using a Hartree-type approximation. The work presented in [34] relies on the assumption that the potential is changing slowly as a function of temperature compared to the motion of the field, so that the temperature can be regarded as frozen at a particular point $T = T_{saddle}$. The fact that their calculation receives contributions from all times explains the difference in rates: for a domain with radius $5 fm$, they estimate that about $90 - 100 \eta'$ -mesons would be produced while our estimate is $4 - 5$ times smaller.

In the above calculations of $N(\vec{k})$ the geometry of the created θ -state is assumed to be a cubical box. For the case of heavy ion collisions, the more realistic case is that of an ellipsoid or elongated rectangular box. We expect the collision to create a region of quark-gluon plasma which has an asymmetry in one direction. In order to model this situation, we evolve a rectangular grid and embed it in a larger square grid and compute the Fourier transform. Once again, we consider the angular averaged value of $N(\vec{k})$.

For a θ -region with dimensions $32 fm \times (8 fm)^2$, we show the spectrum of the η' at the same time slices shown in Fig. 4.4. The side of length $32 fm$ is the direction parallel to the beam direction. The low momentum modes still dominate, but the peak is not as sharp and the higher modes show a stronger presence. Also, since the θ -region is now larger, from Eq.(4.7) we would expect more particles to be created since there is now more energy available. This is evident when comparing Fig. 4.4 with Fig. 4.5. For the two different times shown, we find that $N_{\pi^0} = 0.3$, $N_{\eta} = 12.7$, $N_{\eta'} = 76.3$ for $t = t_1$ and $N_{\pi^0} = 1.7$, $N_{\eta} = 16.8$, $N_{\eta'} = 73.8$ for $t = t_2$.

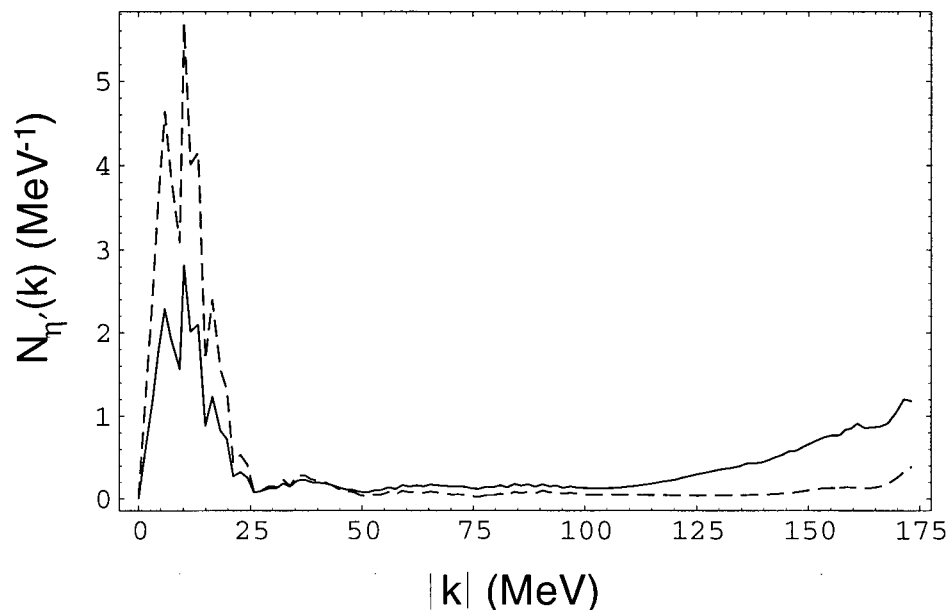


Figure 4.5: The momentum distribution ($N_{\eta'}(k)$ vs. $|\vec{k}|$) is now shown for the case where the geometry of the θ -region is considered as a rectangle. We consider the case where the size of the θ -region is larger along the longitudinal directions compared to the transverse directions. The solid and dotted lines once again represent times $\tau_{shell} = t_1$ and t_2 respectively. Although the majority of the spectrum still exists in the low momentum range, the higher momentum modes now become more evident.

Upon consideration of the above geometry, we must also examine the angular distribution of the system. We choose the coordinates such that the long edge of the θ -region is parallel to the z -axis. In Fig. 4.6, we show the angular distribution of $N_{\pi^0}(\theta)$ as a function of the azimuthal angle θ . This plot suggests that the majority of the particles would have larger momentum components in the direction perpendicular to the beam direction. We also investigated the dependence on the polar angle ϕ and found that there is essentially no dependence, as expected. $N(\vec{k})$ has a constant value which is equal to the peak value in Fig. 4.6.

As was shown in Figures 4.2, 4.3, 4.4, and 4.5, if a θ -vacuum state can be created in heavy ion collisions we should expect an excess of low momentum Goldstone bosons. In particular, the η' would be produced in large amounts. The excess low momentum

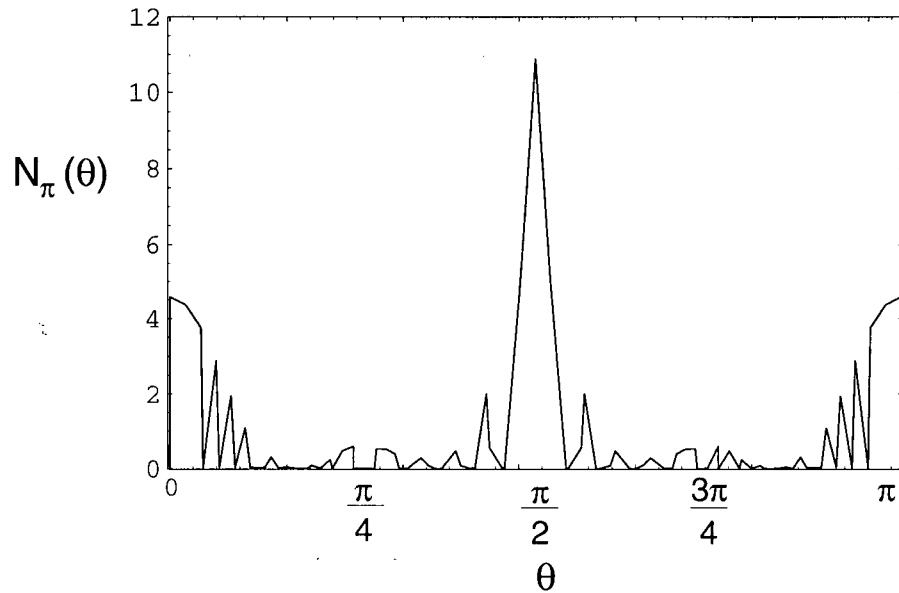


Figure 4.6: For the scenario shown in Fig. 4.5, we consider the angular dependence on the azimuthal angle for the π^0 instead of the η' . The azimuthal angle is defined so that $\theta = 0$ coincides with the beam axis.

π^0 -mesons, η -mesons, and η' -mesons may eventually eventually decay to photons and e^+e^- pairs through such decays as $\pi^0 \rightarrow e^+e^-\gamma$, $\eta \rightarrow e^+e^-\gamma$, and $\eta' \rightarrow e^+e^-\gamma$. The end result would be an excess of long wavelength dileptons, which could possibly provide a solution to the observation of an excess of these particles seen at CERN [3, 4].

Chapter 5

Conclusions and Future Considerations

In this thesis, we provided evidence through numerical simulations of a model based on the Halperin-Zhitnitsky effective potential for QCD that it may be possible to create non-trivial induced θ -vacua in heavy ion collisions. To reiterate, as in [17], we saw an initial growth of the low momentum (long wavelength) modes, followed by damped oscillations. The fact that the only surviving mode is the quasi-zero mode indicates that a nonperturbative condensate has been formed. In addition to this, our hypothesis that the formation of θ -vacua may be possible is supported by the test of independence of volume, as well as the observation of the coarsening phenomenon (amplification of the zero mode with time).

The next logical step would be to ask what kind of signatures should one expect if θ -vacua can be formed in heavy ion collisions. We showed that the creation θ -vacua in heavy ion collisions could result in the amplification of production of light Goldstone bosons in the $(10 - 100) \text{ MeV}$ momentum range. In all calculations, we worked in the instantaneous approximation where the shell separating the θ -state disappears in a time much less than any internal time scale. These low momentum particles would then decay to low momentum photons and dileptons, which could be easily detected. We would like to make the optimistic suggestion that this could possibly account for the unexplained abundance of low momentum dileptons observed at CERN [3, 4].

Our calculations could be extended and improved in several ways. In order to incorporate the effects of expansion, we could introduce a time dependent lattice spacing

$a(t)$. If $a(t)$ increases with time, this will model the dilution of energy in the system. Following an analogy with an expanding universe, the coefficient of the damping term $\dot{\phi}_i$, γ goes like *constant* $\times \dot{a}/a$. Although we have not performed the simulation taking this into account, we can estimate the result as follows. The Laplacian term in Eq.(3.4) is numerically proportional to $1/a$, and if $a(t)$ increases with time, the system will require more time to relax to the θ -state. If the coefficient, γ , is altered as mentioned above and $a(t)$ increases at a constant rate, the damping term will become smaller as time goes on. The overall effect of a time dependent lattice spacing is to increase the formation time of the θ -state.

All calculations relied on the quenched approximation that the system could be evolved according to the zero temperature equations of motion. There exists the possibility that this approximation is not justified. In the case that this proves to be true, we could extend this analysis by introducing non-zero temperature effects. We could also ask how the presence of a non-zero chemical potential would affect our results.

Looking back at Chapter 4, there exists the other possibility that the instantaneous approximation may be the incorrect physical picture. If this process is actually carried out adiabatically, then one must ask what the question: how does the the transformation of the asymptotic states from the $\theta \neq 0$ -world to our world with $\theta = 0$ occur? This presents itself as a very difficult problem which could have interesting results.

Bibliography

- [1] I. Halperin and A. Zhitnitsky. Anomalous effective Lagrangian and θ dependence in QCD at finite N_c . *Phys. Rev. Lett.*, 81:4071, 1998.
- [2] I. Halperin and A. Zhitnitsky. Can θ/N dependence for gluodynamics be compatible with 2π periodicity in θ ? *Phys. Rev.*, D58:054016, 1998.
- [3] G. Agakichiev et al., CERES collaboration. Enhanced production of low-mass electron pairs in 200 GeV/nucleon S-Au collisions at the CERN super proton synchrotron. *Phys. Rev. Lett.*, 75:1272, 1995.
- [4] N. Maserà for the HELIOS-3 collaboration. Dimuon production below mass $3.1 \text{ GeV}/c^2$ in p-W and S-W interactions at 200 GeV/c/A. *Nucl. Phys.*, A590:93c, 1995.
- [5] J.F. Donoghue, E. Golowich, and B.R. Holstein. *Dynamics of the Standard Model*. Cambridge University Press, 1992.
- [6] R.D. Peccei. Reflections on the strong CP problem. *hep-ph/9807514*, 1998.
- [7] J.E. Kim. Light pseudoscalars, particle physics and cosmology. *Phys. Rep.*, 150:1, 1987.
- [8] H.Y. Cheng. The strong CP problem revisited. *Phys. Rep.*, 158:1, 1988.
- [9] R.D. Peccei. In C. Jarlskog, editor, *CP violation*. World Scientific, 1989.
- [10] R. Jackiw and C. Rebbi. Vacuum periodicity in a Yang-Mills quantum theory. *Phys. Rev. Lett.*, 37:172, 1976.
- [11] C. Callan, R. Dashen, and D. Gross. The structure of the gauge theory vacuum. *Phys. Lett.*, B63:334, 1976.
- [12] C. Callan, R. Dashen, and D. Gross. Toward a theory of the strong interactions. *Phys. Rev.*, D17:2717, 1978.
- [13] E. Witten. Large N chiral dynamics. *Ann. Phys.*, 128:363, 1980.
- [14] P. Di Vecchia and G. Veneziano. Chiral dynamics in the large N limit. *Nucl. Phys.*, B171:253, 1980.

- [15] E. Witten. Current algebra theorems for the U(1) Goldstone boson. *Nucl. Phys.*, B156:269, 1979.
- [16] G. Veneziano. U(1) without instantons. *Nucl. Phys.*, B159:213, 1979.
- [17] K. Rajagopal and F. Wilczek. Emergence of coherent long wavelength oscillations after a quench: Application to QCD. *Nucl. Phys.*, B404:577, 1993.
- [18] J.D. Bjorken. A full acceptance detector for SSC physics at low and intermediate mass scales: An expression of interest to the SSC. *Int. J. Mod. Phys.*, A7:4189, 1992.
- [19] A.A. Anselm and M.G. Ryskin. Production of classical pion field in heavy ion high-energy collisions. *Phys. Lett.*, B266:482, 1991.
- [20] J.P. Blaizot and A. Kryzwicki. Soft pion emission in heavy ion high-energy collisions. *Phys. Rev.*, D46:246, 1992.
- [21] K. Rajagopal. The chiral phase transition in QCD: Critical phenomena and long wavelength pion oscillations, hep-ph/9504310. In R. Hwa, editor, *Quark-Gluon Plasma 2*, page 484. World Scientific, 1995.
- [22] K. Buckley T. Fugleberg and A. Zhitnitsky. Can θ vacua be created in heavy ion collisions? *Phys. Rev. Lett.*, 84:4814, 2000.
- [23] T. Fugleberg, I. Halperin, and A. Zhitnitsky. Domain walls and θ dependences in QCD with an effective Lagrangian approach. *Phys. Rev.*, D59:074023, 1999.
- [24] A. Zhitnitsky. Signatures of the induced θ vacuum state in heavy ion collisions. *hep-ph/0003191*, 2000.
- [25] K. Buckley T. Fugleberg and A. Zhitnitsky. Induced θ -vacua in heavy ion collisions: A possible signature. *hep-ph/0006057*, 2000.
- [26] A. Kovner and M. Shifman. Chirally symmetric phase of supersymmetric gluodynamics. *Phys. Rev.*, D56:2396, 1997.
- [27] R.J. Crewther. Chirality selection rules and the U(1) problem. *Phys. Lett.*, 70B:349, 1977.
- [28] M.A. Shifman, A.I. Vainshtein, and V.I. Zakharov. Can confinement ensure natural CP invariance of strong interactions? *Nucl. Phys.*, B166:493, 1980.
- [29] D. Boyanovsky and H.J. de Vega. Dynamics of symmetry breaking out of equilibrium: From condensed matter to QCD and the early Universe. *hep-ph/9909372*, 1999.

- [30] I. Halperin and A. Zhitnitsky. Axion potential, topological defects and CP-odd bubbles in QCD. *Phys. Lett.*, B440:77, 1998.
- [31] W. Press, S. Teukolsky, W. Vetterling, and B. Flannery. *Numerical Recipes in C*. Cambridge University Press, 1992.
- [32] D. Kharzeev, R. Pisarski, and M. Tytgat. Possibility of spontaneous parity violation in hot QCD. *Phys. Rev. Lett.*, 81:512, 1998.
- [33] D. Kharzeev and R. Pisarski,. Pionic measures of parity and CP violation in high-energy nuclear collisions. *Phys. Rev.*, D61:111901, 2000.
- [34] D. Ahrensmeier, R. Baier, and M. Dirks. Resonant decay of parity odd bubbles in hot hadronic matter. *hep-ph/0005051*, 2000.